

Article

Immobilized TiO₂-Polyethylene Glycol: Effects of Aeration and pH of Methylene Blue Dye

Wan Izhan Nawawi ^{1,*}, Raihan Zaharudin ^{1,2}, Ahmad Zuliahani ¹, Dyia Syaleyana Shukri ¹, Tun Firdaus Azis ¹ and Zainab Razali ¹

¹ Faculty of Applied Sciences, Universiti Teknologi MARA, Perlis, Arau 02600, Malaysia; nurraihanzaharudin@gmail.com (R.Z.); zuliahani@perlis.uitm.edu.my (A.Z.); dyia839@perlis.uitm.edu.my (D.S.S.); firdausbinazis@gmail.com (T.F.A.); zainab215@perlis.uitm.edu.my (Z.R.)

² Faculty of Applied Sciences, Universiti Teknologi MARA, Selangor, Shah Alam 40450, Malaysia

* Correspondence: wi_nawawi@perlis.uitm.edu.my; Tel.: +60-49-882-305; Fax: +60-49-882-304

Academic Editor: Rajender S. Varma

Received: 24 February 2017; Accepted: 4 May 2017; Published: 12 May 2017

Abstract: Immobilized TiO₂ and immobilized TiO₂-polyethylene glycol (TiO₂/PEG) films have been prepared via brush coating method. The formulation of immobilized TiO₂ film was prepared by mixing distilled water with P25, while the formulation containing P25 combined with 8% PEG in distilled water was used in preparing immobilized TiO₂/PEG. A double sided adhesive tape (DSAT) was stacked onto a glass surface prior to coating with the formulations and annealing by a thermal treatment at 100 °C for 15 min. The photocatalytic activity of immobilized photocatalysts was evaluated under photodegradation of methylene blue (MB). It was observed that immobilized TiO₂/PEG has showed a higher rate of photocatalytic activity compared to immobilize TiO₂. The X-ray photoelectron spectroscopy and Fourier transform infrared (FT-IR) spectra of immobilized TiO₂/PEG sample proved that the existence of C=O led to enhanced photoactivity efficiency under normal light and visible light irradiations. The photocatalytic activity performance of immobilized TiO₂/PEG was the highest at 75 mL·min^{−1} aeration rate and pH 11 of MB dye. The correlation between of all these parameters was investigated in this study.

Keywords: immobilized TiO₂; polyethylene glycol; double sided adhesive tape; methylene blue dye

1. Introduction

Dye pollutants or effluents have attracted wide attention due to their toxicity and resistance for removal-feature. It has been a challenging task to decompose these effluents (e.g., methylene blue (MB) dye) [1,2]. Some of the major works conducted on MB dye were in aqueous solutions using photocatalysis method, and some of these photocatalytic studies were also employed in immobilization systems [3–6]. In aqueous systems such as slurry or suspension method, photocatalysts require an expensive photocatalyst recovery process which limits its application due to high scale-up cost and because it is not environmentally friendly [7,8]. Even though there are several commercial photocatalysts available, the TiO₂ photocatalyst is always an option used in photocatalysis such as in wastewater remediation due to its high performance, low equipment cost, and low toxicity [9,10]. Alternatively, immobilization of TiO₂ has been explored, and displayed better catalytic compared to TiO₂ suspension [11]. Moreover, a comprehensive review of TiO₂ films was conducted by Varshney et al. (2016), in which various types of coating methods (e.g., doctor-blade, chemical vapour deposition, hydrothermal, electrophoretic deposition, sputter deposition, spray pyrolysis, and flame aerosol coating methods) are thoroughly explained [12]. In an earlier study by Sökmen et al. [13], immobilized TiO₂ was used for the photodegradation of MB dye. This study revealed that more MB dye was

removed in a shorter amount of time through immobilized TiO₂–polymer. Studies have shown that the incorporation of polymer such as polyethylene glycol (PEG) in photocatalysis is highly beneficial for the enhancement of the catalytic activity of the immobilized sample. PEG is a polymeric material that can be employed to boost the functionalization of TiO₂ surface which acted as a matrix agent or as a structure directing agent [14–16].

Ćurković et al. [17] claimed that immobilized TiO₂ with PEG exhibited higher catalytic activity and achieved higher surface density compared to other immobilized sample without the addition of PEG. The addition of PEG was proven to create a remarkable porosity in immobilized TiO₂ sample [18]. It has been realized that the size of pores increased with increased molecular weight of PEG [19]. This factor indirectly promotes an excellent performance of immobilized photocatalyst sample. In another study by Liu et al. [20], the addition of high molecular weight PEG (i.e., PEG 6000) presented a major increase in specific surface area, well-defined particle size, and enhanced photo-generated charge separation rate between conduction band (CB) and valence band (VB) during oxidation process. Meanwhile, studies have shown that adhesive tapes (e.g., scotch tape, double sided adhesive tape (DSAT), and hatch tape) were previously used to measure the adhesiveness of TiO₂ films onto substrate [21,22]. However, the functionalization of adhesive tapes (i.e., DSAT) as a support binder has not been studied extensively. Besides, improving the adherence of TiO₂ film with flat supports such as glass plates is crucial to obtain an optimal photocatalytic effect. This is because film adhesion is one of the biggest challenges in polymer-immobilized photocatalyst [23]. Based on our previous works [24,25], DSAT was not only proven to strengthen the adhesion of TiO₂ film to glass plate, but also improved the reusability of immobilized photocatalyst for up to 30 cycles. The immobilized TiO₂–DSAT successfully demonstrated an outstanding photocatalytic activity on the decolorization of Reactive Red 4 (RR4) and methylene blue dye. During the 30 cycles, the photocatalyst sample maintained a high photodegradation rate, indicating good stability of immobilized TiO₂–DSAT. Therefore, in this study, efforts have been made to immobilize TiO₂ photocatalyst with pore matrix PEG 6000 and DSAT as a thin layer binder. The immobilization system utilized a paint brush-coating technique with low heat treatment method. The MB dye was used as a target pollutant in aqueous media to assess the photocatalytic activity. This study serves as an extension of our immobilization reports [26]; thus, the influence of experimental parameters such as aeration flow rate, initial dye concentration, and effect of pH were also investigated.

2. Experimental

2.1. Preparation of Immobilized TiO₂/PEG and TiO₂ Films

Based on previous works [21], the immobilized TiO₂/PEG was prepared by dissolving 6.5 g of titanium dioxide (TiO₂) Degussa P25 powder in 50 mL of distilled water added with 1 mL of 8% (w/v) of polyethylene glycol (PEG) solution (Merck, Darmstadt, Germany, molecular weight (MW) = 6000). The sample solution was thoroughly shook through a sonication process for one hour, producing a homogenized formulation. The sample films were prepared by using a brush-coating method applied onto glass substrates [24,25], which were cleaned and taped with double-sided adhesive tape (DSAT) prior to coating. The coated glass was then dried using a hot air blower at 100 °C for 15 min. The thickness of the immobilized films was controlled by the optimal amount of photocatalyst loading and number of coatings [27]. The same procedure was repeated for immobilized TiO₂ with the exception of the addition of PEG.

2.2. The Washing Process of Immobilized Samples and Photoactivity Test under Different Light Conditions

The cleaning process was conducted to remove all unwanted contaminants by irradiating the immobilized samples using distilled water. The washing process was carried out for one hour under normal light (NL) irradiation to increase the permeability performance prior to photoactivity test. The photoactivities of the immobilized samples were tested by degradation of methylene blue (MB; Fluka Analytical, St. Louis, MO, USA). The experimental setup used was to apply immobilized

sample with 20 mL of 12 mg/L concentration of MB dye into a glass cell (dimension: 50 mm length \times 10 mm width \times 80 mm height). An NS 7200 aquarium pump was used as an aeration source along the photodegradation process. Area of photocatalytic activity is equal to length \times width of DSAT applied, which is 6.6 cm \times 4.6 cm. The photoactivity tests of the immobilized samples were conducted under normal light and visible light (VL) irradiation. The NL intensity of the lamp used was measured at about 461 and 6.7 W/m² for visible and UV lights, respectively, while an intensity of 430 W/m² was used for VL source. Turning on the 55-W compact fluorescent lamp as the normal light source as shown in Figure 1 initiated the photocatalytic reaction, and outlet absorbance was measured. A 4 mL aliquot was extracted from the glass cell reactor at pre-specified intervals. The absorbance of the aliquot was measured by a UV spectrophotometer (Varian UV-Vis detector model HACH DR 1900, HACH, Loveland, CO, USA) set to 661 nm, which corresponds to the MB absorbance. MB concentration trends were simulated using a pseudo first-order rate constant plot of $\ln(C_0/C_t) = kt$, where C_0 represents the MB concentration at $t = 0$ min, C_t is the concentration at time t , and k is kinetic constant or photoactivity efficiency at min⁻¹. The concentration of MB at different experimental times was spectrometrically evaluated [28]. The final MB concentration can be spectrometrically determined with a calibration curve using the Beer–Lambert equation, which is $A = l\varepsilon[\text{MB}]$, where l is the path length, $[\text{MB}]$ is the concentration of the dye, and ε is the MB molar absorptivity [27]. For VL irradiation, a glass cell that contained MB solutions was exposed to the visible light from a 55-W fluorescent lamp attached with a UV filter (>420 nm) at room temperature conditions. With the pseudo first-order plot, absorbance was converted to concentration, and rate of degradation (k) was calculated.

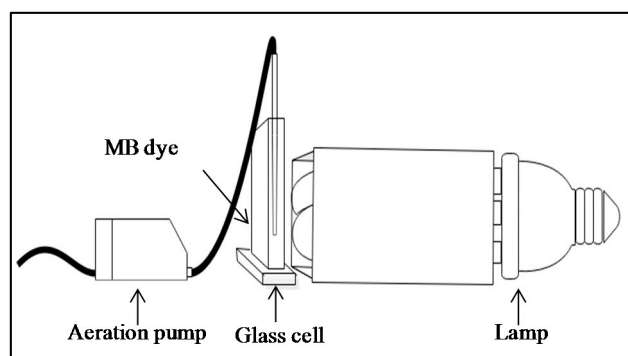


Figure 1. The photoactivity test of methylene blue (MB) dye for immobilized TiO₂ and TiO₂/PEG. PEG: polyethylene glycol.

2.3. Characterization of Immobilized Samples Using Fourier Transform Infrared Spectroscopy (FT-IR) and X-ray Photoelectron Spectroscopy (XPS)

FT-IR spectra of immobilized TiO₂ and TiO₂/PEG samples in powder form were analysed on Perkin Elmer Spectrum Version equipped with an attenuated total reflectance device (Frontier, Waltham, MA, USA) with a diamond crystal. Spectra were collected in a wavelength range of 600–4000 cm⁻¹ with four scans and spectral resolution of 4 cm⁻¹. The binding energy of immobilized TiO₂/PEG was determined using X-ray photoelectron spectroscopy (XPS) with a Thermo ESCALAB 250 spectrometer (Thermo Fisher Scientific, Waltham, MA, USA) using a radiation source of monochromatic Al K α with the energy of 1486.6 eV.

2.4. Effects of Aeration and Initial pH Condition

The photocatalytic study of immobilized samples in the degradation of MB dye as a model pollutant was studied under different parameters (i.e., different aeration rate, pH, and initial condition). The photocatalytic degradation studies for all parameters are based on the previous Section 2.2. Four different air flow rates (25, 50, 75, and 100 mL·min⁻¹) were used to study the effect of aeration rate. Under NL irradiation, the effect of pH was investigated by irradiating an immobilized TiO₂/PEG

sample using different pHs of MB dye solutions (pH 3, 6, 8, 10, 11, and 12). Hydrochloric acid (HCl) and sodium hydroxide (NaOH) were used to change the pH of MB solution. Four MB solutions with different concentrations were used (6, 12, 24, and 36 ppm) for initial concentration test. The solutions were subjected to an adsorption process to observe the initial degradation rate. The determination of the pH of the zero charge was conducted by adding a 0.01 g of unmodified TiO₂ and modified TiO₂/PEG powder into several 50 mL of pH-adjusted ultra-pure water solutions ranging from pH 2 to 10 followed by the addition of 10 mL of 0.1 M KCl. The solutions were stirred, and the final pH values were recorded after 24 h of stirring. The discrepancies of the pH were obtained by subtracting the initial pH with the final pH. A plot of pH discrepancies versus the initial pH was constructed, and the point of zero charge was obtained from the values which cut the *x*-axis. The degradation of MB (concentration against time) was presented according to pseudo first-order rate constant plot.

3. Result and Discussion

3.1. FT-IR and XPS Analysis of Immobilized TiO₂ and TiO₂/PEG

The FT-IR spectra of immobilized TiO₂ and TiO₂/PEG were determined and are presented in Figure 2a. The spectra revealed a strong and sharp absorption peak at 1705.02 cm⁻¹ which is attributable to the existence of C=O bond in immobilized TiO₂/PEG sample. At the lower wavenumber of 1160.06 cm⁻¹, another bond was discovered corresponding to the stretching vibration of carbonyl oxygen or the C–O bond. However, the C=O and C–O bonds were not found in the immobilized TiO₂ sample. These newly-discovered peaks observed in immobilized TiO₂/PEG were the result of the introduction of high molecular weight PEG 6000 into the immobilized sample. The oxidation of PEG 6000 in washed film was detected owing to the strong absorption by the carbonyl group in the FT-IR spectrum [29]. The strong absorption peaks of C=O and C–O bonds represent a successful interaction of TiO₂ nanoparticles with PEG 6000 that favours good photocatalytic activity, as shown previously. The surface analysis of immobilized TiO₂/PEG was also studied by X-ray photoelectron spectroscopy, as displayed in Figure 2b.

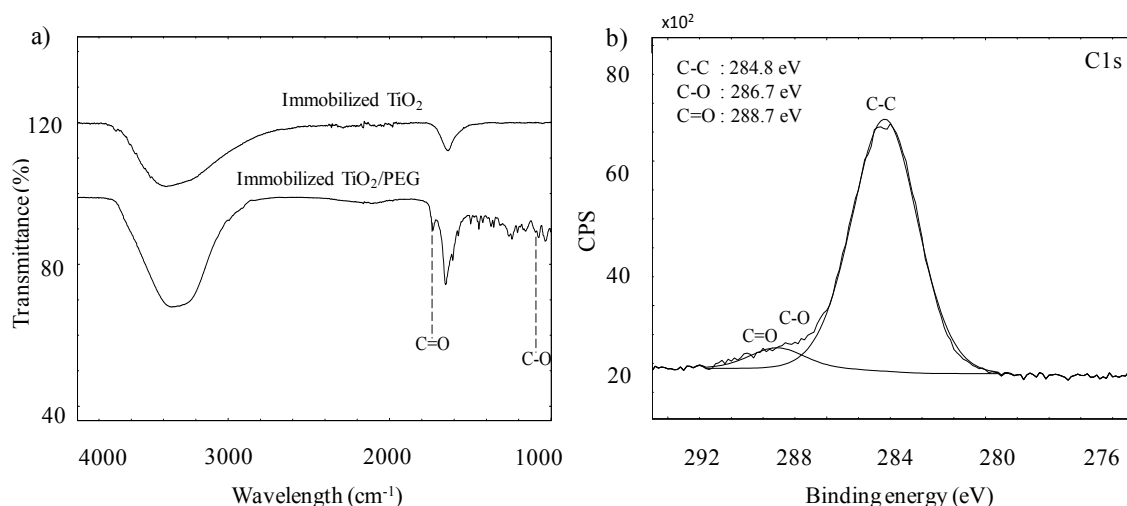


Figure 2. The spectrum for: (a) the Fourier transform infrared spectroscopy (FT-IR) for immobilized TiO₂ and TiO₂/PEG samples; and (b) X-ray photoelectron spectroscopy (XPS) deconvolution peaks of C1s for immobilized TiO₂/PEG.

In this study, the C1s spectra of XPS analysis revealed the significant presence of a C=O bond according to its characteristic binding energy at 288.7 eV. Other peaks detected were found to be C–O bond and C–C bond observed at 286.7 and 284.8 eV, respectively. This finding is very important because C=O and C–O bonds were the two main species responsible for the wider photoactivity response

of TiO_2 photocatalyst in the VL spectrum [30]. Due to the C=O and C–O bonds in immobilized TiO_2/PEG , the immobilized sample is able to have a good photoactivity efficiency under both NL and VL irradiation. The bonds act as electron injectors that speed up the photodegradation process when they are adsorbed on TiO_2 surface and become excited by VL. From here, new electrons are formed and are injected to the conduction band of the TiO_2 photocatalyst. The conduction band transferred the electrons from the bonds to electron acceptors on the immobilized TiO_2/PEG surface. The excited electrons in the conduction band then performed a series of chain reactions that contribute to enhanced performance of immobilized TiO_2/PEG under VL spectrum.

3.2. Photoactivity Tests of Immobilized TiO_2 and TiO_2/PEG under Different Light Irradiations

The degradation of MB dye under NL and VL irradiations was used to study the photocatalytic activity of immobilized TiO_2 and TiO_2/PEG samples. Under identical conditions, it was found that only 18.7% of MB dye solution was adsorbed on the immobilized TiO_2 in the dark after 30 min, while the amount of MB removed by the TiO_2/PEG was 47.4% [26]. This suggests that the greater adsorption of MB on TiO_2/PEG as compared to immobilized TiO_2 is attributed to the higher surface area of TiO_2/PEG (Brunauer–Emmett–Teller (BET) surface area of the photocatalysts: TiO_2/PEG , $88 \text{ m}^2/\text{g}$; TiO_2 , $49 \text{ m}^2/\text{g}$). As can be seen in Figure 3a, the immobilized TiO_2/PEG sample exhibited higher photocatalytic activities than immobilized TiO_2 under NL irradiation, with the dye remaining for immobilized TiO_2/PEG being 0.29 as compared to 0.58 for immobilized TiO_2 in 15 min of irradiation time. At this stage, the photoactivity efficiency of immobilized TiO_2 was proven to be two times better than immobilized TiO_2 . The high photoactivity efficiency rate of immobilized TiO_2/PEG can first be attributed to the synergistic effect of adsorption and photocatalysis [27]. Results revealed that the enlarged surface area was dominant in the TiO_2/PEG film and was found to be twice as large as the latter. The washings of immobilized TiO_2/PEG film improved the photocatalytic ability in degrading the MB under NL illumination. Through the photooxidation process in washing, the PEG became oxidized and created more pores and active sites on the TiO_2 surface. Thus, the photoactivity efficiency rate for immobilized TiO_2/PEG was found to be 0.065 min^{-1} , and 0.055 min^{-1} for immobilized TiO_2 . It is obvious that the k value for immobilized TiO_2/PEG is 1.2 times higher than the immobilized TiO_2 sample.

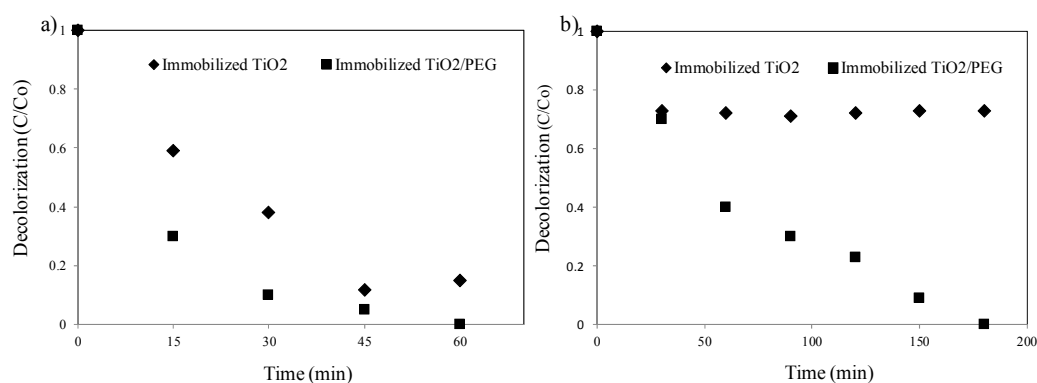


Figure 3. Immobilized TiO_2 and TiO_2/PEG sample for MB photodegradation under: (a) normal light irradiation and (b) visible light irradiation at $\text{MB}_0 = 12 \text{ ppm}$, pH 11, 28°C .

In addition, the decolorization for immobilized TiO_2 under VL irradiation was nearly a straight line, as presented in Figure 3b. Through the pseudo first-order equation, the photoactivity efficiency rate of immobilized TiO_2/PEG was found to be 0.012 min^{-1} . This result is in contrast to immobilized TiO_2 photocatalyst, where it was inactive under VL irradiation due to its large band gap energy. From Figure 3b, the dye remaining for immobilized TiO_2/PEG was colourless in only 180 min of irradiation. Compared to immobilized TiO_2 , the remaining MB was found to be 0.75 in the same

conditions. Thus, the immobilized TiO_2/PEG sample performed better photodegradation as compared to immobilized TiO_2 under VL spectrum. This is mainly because of the presence of $\text{C}=\text{O}$ and $\text{C}-\text{O}$ bonds that contributed to the VL response ability in immobilized TiO_2/PEG .

3.3. Effects of Aeration Rate

Aeration flow rate affects the photoactivity efficiency of immobilized TiO_2/PEG because it acts as an oxygen supply for the photocatalyst [31]. The effect of aeration flow rate was identified based on first-order rate constant (k) value against flow rate and is shown in Table 1, and decolorization (C/C_0) is shown in Figure 4, respectively. With PEG and DSAT in immobilized TiO_2/PEG , the concentration of MB dropped from 12 to 0 ppm in one hour with the highest removal efficiency rate at 75 mL/min. As can be seen in Figure 4, the dye remaining was up to 0.29 in just 15 min as compared to 0.53, 0.36, and 0.62 for 100, 50, and 25 mL/min aeration, respectively. The value of photodegradation efficiency (k) at 0.0347, 0.058, 0.068, and 0.053 min^{-1} for 25, 50, 75, and 100 mL/min flow rate accordingly indicates that the photocatalytic degradation of MB increased with increased aeration up to 75 mL/min; beyond that, however, the k value dropped by 0.22 to become 0.053 min^{-1} at 100 mL/min. In other words, at 75 mL/min, optimum flow rate for photodegradation of MB reached as high as 0.068 min^{-1} of removal efficiency. High aeration flow rate supply produced a high oxygen concentration and reacted with excited electrons from photon flux, producing O_2^- anions. The production of O_2^- caused the photodegradation rate of MB to increase as the aeration flow rate increased [32]. However, the excessive flow rate beyond 75 mL/min affected the penetration of light due to the production of a huge amount of bubbles during the photocatalysis irradiation.

Table 1. The kinetic constants (k) of decolorizing MB at different aeration flow rates for optimum loading of 0.3 g of immobilized TiO_2/PEG .

Aeration (mL/min)	k , Rate Constant (min^{-1})	Correlation Coefficient (R^2)
25	0.035	0.9969
50	0.058	0.9950
75	0.068	0.9913
100	0.053	0.9940

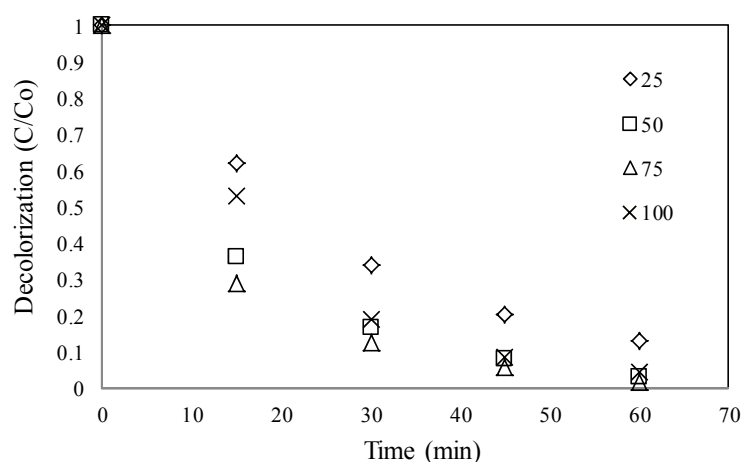


Figure 4. Aeration flow rate (mL/min) of immobilized TiO_2/PEG photocatalyst film.

3.4. Effects of pH

Researchers have paid much attention to studying the effect of pH on the photocatalytic degradation of dyes because the real wastewater effluences from industries may not have a neutral pH (pH 7). Moreover, the pH of the reaction mixture influences the surface-charged- properties of

the photocatalysts. The effect of pH is important to study, as it impacts the surface state of titanium and the ionization state of the dye molecules [33]. In this study, the effect of pH on MB degradation was evaluated at various pH conditions (i.e., 3, 6, 8, 10, 11, and 12). The significant effect of pH on the calculated pseudo first-order rate constant for the photocatalytic decolourization of MB is depicted in Figure 5a. It was observed that the photocatalytic degradation rate increased by increasing the pH value. pH 11 showed the highest photocatalytic activity as compared to other pH. This is also due to the significant effect of high adsorption existing between positively-charged cationic MB dye with the negative charge on the surface of immobilized TiO_2/PEG . As can be seen in Figure 5, there is a difference in the values of MB photodegradation rate between pH 4 and pH 8. Figure 5b shows the plot graph of the pH value corresponding to the point of zero charge (pH_{pzc}) of immobilized TiO_2/PEG surface where the value of pH_{pzc} is 6.5. This means that the surface charge of immobilized TiO_2/PEG is positive in acidic pH ($\text{pH} < 6.5$) and negatively charged in alkaline pH ($\text{pH} > 6.5$). The pH_{pzc} is a pH value where the net electrical charge of the photocatalyst is zero and is used to qualitatively assess the TiO_2 surface charge. Due to the negatively-charged TiO_2/PEG surface in alkaline conditions, adsorption dominates between the negative TiO_2 surface and the cationic MB dye ($\text{p}K_{\text{a}} < 2$) [34]. Hence, a pH value lower than 6.5 will cause a poor degradation of MB dye, and this explains the gap in photocatalytic degradation rate obtained beyond pH 6.5 seen in Figure 5b. However, the photoactivity efficiency decreased at pH 12 to become 0.062 min^{-1} due to the rapid adsorption of dye which covered the photocatalyst surface, thus resulting in a slower photocatalytic activity [35]. Nonetheless, the removal rate of MB by TiO_2/PEG film was largely attributed to adsorption, since the visible blue-stained surface indicated that the film was not fully photocatalytically degraded. This is due to the agglomeration of MB, which reduced the amount of light needed for photocatalysis [36]. Thus, the optimal pH obtained in this study was discovered to be at pH 11.

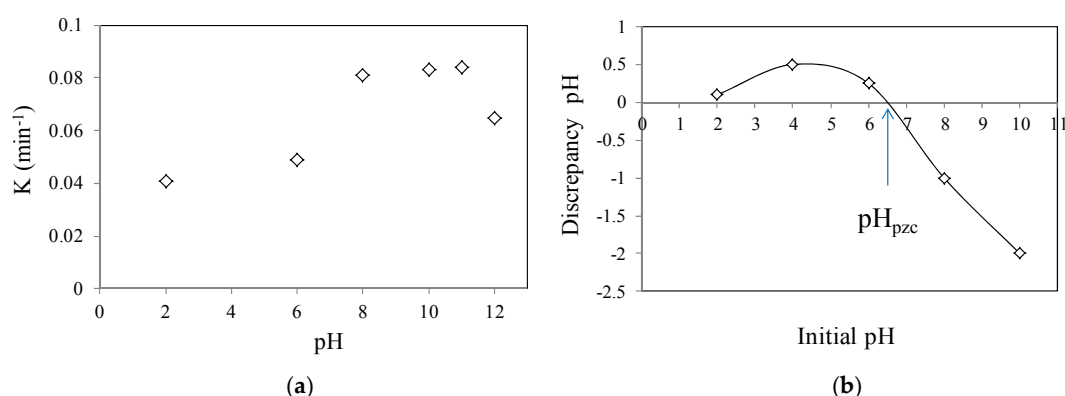


Figure 5. Immobilized TiO_2/PEG photocatalyst film for: (a) Initial pH effect and (b) plot of the pH value corresponding to the point of zero charge.

4. Conclusions

In our study, immobilized TiO_2/PEG best demonstrated its properties in normal light applications at $75 \text{ mL} \cdot \text{min}^{-1}$ aeration and pH 11. Due to the C=O and C–O bonds found in immobilized TiO_2/PEG , the photoactivity tests were well performed under NL and VL irradiation. The bonds accelerated the photoactivity efficiency by acting as an electron injector. It was also found that the presence of PEG and DSAT assisted in the high removal efficiency of MB dye due to the ease of usage and good photocatalytic activity, as reported in our previous study. The findings promised a potent feasible application in photocatalysis regarding the simple deposition method as well as the incorporation of a pore matrix polymer like PEG. For future recommendation, some works will be developed to enhance the photocatalytic ability of immobilized TiO_2/PEG sample. First, the mechanism of PEG-DSAT will be studied as to why and how the C–O in PEG turned to a C=O bond. Then, the effect of sintering or calcination under elevated temperature will also be conducted. It is also necessary to further exploit the

bulk properties modification of TiO₂/PEG DSAT, and further study of its overall kinetic and adsorption isotherm would be beneficial. Next, the novel low heat-brush coating method will be re-adopted in order to create a smooth and uniform layer of immobilized TiO₂/PEG before further implementation in an industrial reactor such as semi-batch photocatalytic reactor [37]. The increased specific surface area of PEG 6000 in immobilized TiO₂/PEG should contribute to a closer and full contact of dye pollutant with the photocatalyst sample; hence, enhancing the efficiencies of photo-generated charge carriers should effectively improve the photocatalysis performance [38]. Therefore, the effect of different flat supports (e.g., graphite plate, stainless steel plate, and ceramic plate) on the photocatalysis performance of immobilized TiO₂/PEG will be studied. Under suitable conditions, the utilization of graphite plate could possibly trigger a photo-electro-catalytic process in immobilized TiO₂/PEG, which is more powerful than a conventional oxidation method [39]. Studies on the photodegradation of a complex molecule (i.e., phenol) as a general pollutant in real waste water is also essential to expand the application of immobilized TiO₂/PEG to a wider range of situations, instead of one specific readily-oxidized pollutant and its by-products [40]. It also becomes of great importance to explore the existence of other species in immobilized TiO₂/PEG (i.e., C=C) that may contribute to an expanded photo response from ultraviolet (UV) spectrum to VL spectrum of TiO₂ photocatalyst [41].

Acknowledgments: We would like to thanks the Malaysian Ministry of Education (KPM) for providing generous financial support under REI grants: 600-IRMI/DANA 5/3/REI (1/2017) in conducting this study and Universiti Teknologi Mara (UiTM) for providing all the needed facilities.

Author Contributions: The experimental work and drafting of the manuscript was carried out by Raihan Zaharudin and assisted by Dyia Syaleyana Shukri, Tun Firdaus Azis, Zainab Razali and Ahmad Zuliahani participated in the interpretation of the scientific results and the preparation of the manuscript. Wan Izhan Nawawi supported the work and cooperation between UiTM Perlis and UiTM Shah Alam, supervised the experimental work, commented and approved the manuscript. The manuscript was written through comments and contributions of all authors. All authors have given approval to the final version of the manuscript.

Conflicts of Interest: The authors declare no conflict of interest.

References

1. Ali, R.; Siew, O.B. Photodegradation of new methylene blue N in aqueous solution using zinc oxide and titanium dioxide as catalyst. *J. Teknol.* **2007**, *45*, 31–41. [[CrossRef](#)]
2. Joshi, K.; Shrivastava, V. Removal of methylene blue dye aqueous solution using photocatalysis. *Int. J. Nano Dimens.* **2012**, *2*, 241–252.
3. Zhang, W.J.; Li, K.X.; Bai, J.W. Methyl orange photoelectrocatalytic degradation using porous TiO₂ film electrode in NaH₂PO₄ solution. *Adv. Mater. Res.* **2012**, *433–440*, 411–415.
4. Wang, J.; Li, C.; Zhuang, H.; Zhang, J. Photocatalytic degradation of methylene blue and inactivation of gram negative bacteria by TiO₂ nanoparticles in aqueous suspension. *Food Control* **2013**, *34*, 372–377. [[CrossRef](#)]
5. Barakat, M.A. Adsorption and photodegradation of Procion yellow H-EXL dye in textile wastewater over TiO₂ suspension. *J. Hydro-Environ. Res.* **2011**, *5*, 137–142. [[CrossRef](#)]
6. Petrella, A.; Mascolo, G.; Murgolo, S.; Petruzzelli, V.; Ranieri, E.; Spasiano, D.; Petruzzelli, D. Photocatalytic oxidation of organic micro-pollutants: Pilot plant investigation and mechanistic aspects of the degradation reaction. *Chem. Eng. Commun.* **2016**, *203*, 1298–1307. [[CrossRef](#)]
7. Quiñones, C.; Ayala, J.; Vallejo, W. Methylene blue photoelectrodegradation under UV irradiation on Au/Pd-modified TiO₂ films. *Appl. Surf. Sci.* **2010**, *257*, 367–371. [[CrossRef](#)]
8. Meena, R.C. A study on rate of decolorization of textile azo dye Direct Red 5B by recently developed photocatalyst. *Int. J. Sci. Res. Publ.* **2013**, *3*, 5–8.
9. Chong, M.N.; Jin, B.; Chow, C.W.K.; Saint, C. Recent developments in photocatalytic water treatment technology: A review. *Water Res.* **2010**, *44*, 2997–3027. [[CrossRef](#)] [[PubMed](#)]
10. Khodadadi, B.; Sabeti, M.; Moradi, S.; Azar, P.A.; Farshid, S.R. Synthesis of Cu-TiO₂ nanocomposite and investigation of the effectiveness of PEG, pectin and CMC as additives. *J. Appl. Chem. Res.* **2012**, *20*, 36–44.
11. Mascolo, G.; Comparelli, R.; Curri, M.L.; Lovecchio, G.; Lopez, A.; Agostiano, A. Photocatalytic degradation of methyl red by TiO₂: Comparison of the efficiency of immobilized nanoparticles versus conventional suspended catalyst. *J. Hazard. Mater.* **2007**, *142*, 130–137. [[CrossRef](#)] [[PubMed](#)]

12. Varshney, G.; Kanel, S.R.; Kempisty, D.M.; Varshney, V.; Agrawal, A.; Sahle-Demessie, E.; Varma, R.S.; Nadagouda, M.N. Nanoscale TiO₂ films and their application in remediation of organic pollutants. *Coord. Chem. Rev.* **2016**, *306*, 43–64. [[CrossRef](#)]
13. Sökmen, M.; Tatlidil, I.; Breen, C.; Clegg, F.; Buruk, C.K.; Sivlim, T.; Akkan, Ş. A new nano-TiO₂ immobilized biodegradable polymer with self-cleaning properties. *J. Hazard. Mater.* **2011**, *187*, 199–205. [[CrossRef](#)] [[PubMed](#)]
14. Chang, H.; Jo, E.H.; Jang, H.D.; Kim, T.O. Synthesis of PEG-modified TiO₂-InVO₄ nanoparticles via combustion method and photocatalytic degradation of methylene blue. *Mater. Lett.* **2013**, *92*, 202–205. [[CrossRef](#)]
15. Milanovic, M.; Nikolic, L.M. Modification of TiO₂ nanoparticles through lanthanum doping and PEG templating. *Process. Appl. Ceram.* **2014**, *8*, 195–202. [[CrossRef](#)]
16. Singh, S.; Mahalingam, H.; Singh, P.K. Polymer-supported titanium dioxide photocatalysts for environmental remediation: A review. *Appl. Catal. A* **2013**, *462*, 178–195. [[CrossRef](#)]
17. Ćurković, L.; Ljubas, D.; Šegota, S.; Bačić, I. Photocatalytic degradation of Lissamine Green B dye by using nanostructured sol-gel TiO₂ films. *J. Alloys Compd.* **2014**, *604*, 309–316. [[CrossRef](#)]
18. Hutanu, D.; Frishberg, M.D.; Guo, L.; Darie, C.C. Recent applications of polyethylene glycols (PEGs) and PEG derivatives. *Mod. Chem. Appl.* **2014**, *2*, 1–6. [[CrossRef](#)]
19. Guo, B.; Liu, Z.; Hong, L.; Jiang, H.; Lee, J.Y. Photocatalytic effect of the sol-gel derived nanoporous TiO₂ transparent thin films. *Thin Solid Films* **2005**, *479*, 310–315. [[CrossRef](#)]
20. Liu, X.; Zhong, J.; Li, J.; Huang, S.; Song, W. PEG-assisted hydrothermal synthesis of BiOCl with enhanced photocatalytic performance. *Appl. Phys. A* **2015**, *119*, 1203–1208. [[CrossRef](#)]
21. Chen, Y.; Dionysiou, D.D. A Comparative study on physicochemical properties and photocatalytic behavior of macroporous TiO₂-P25 composite films and macroporous TiO₂ films coated on stainless steel substrate. *Appl. Catal. A* **2007**, *317*, 129–137. [[CrossRef](#)]
22. Schäffer, J. Immobilization of TiO₂: Via different routes for photocatalytic reactions in a PDMS based microreactor. Bachelor's Thesis, University of Twente, Enschede, The Netherlands, 2012.
23. Langlet, M.; Kim, A.; Audier, M.; Herrmann, J.M. Sol-gel preparation of photocatalytic TiO₂ films on polymer substrates. *J. Sol-Gel Sci. Technol.* **2002**, *25*, 223–234. [[CrossRef](#)]
24. Ismail, W.I.N.W.; Ain, S.K.; Zaharudin, R.; Jawad, A.H.; Ishak, M.A.M.; Sahid, S. New TiO₂/DSAT immobilization system for photodegradation of anionic and cationic dyes. *Int. J. Photoenergy* **2015**, *2015*, 232741. [[CrossRef](#)]
25. Zaharudin, R.; Azami, M.S.; Ain, S.K.; Bakar, F.; Nawawi, W.I. A comparison study of new TiO₂ immobilized techniques under normal and visible light irradiations. *MATEC Web Conf.* **2016**, *47*, 05017. [[CrossRef](#)]
26. Nawawi, W.; Zaharudin, R.; Ishak, M.; Ismail, K.; Zuliahani, A. The preparation and characterization of immobilized TiO₂/PEG by using DSAT as a support binder. *Appl. Sci.* **2016**, *7*, 24. [[CrossRef](#)]
27. Nawi, M.A.; Sabar, S. Photocatalytic decolourisation of Reactive Red 4 dye by an immobilised TiO₂/chitosan layer by layer system. *J. Colloid Interface Sci.* **2012**, *372*, 80–87. [[CrossRef](#)] [[PubMed](#)]
28. Šuligoj, A.; Štangar, U.L.; Ristić, A.; Mazaj, M.; Verhovšek, D.; Tušar, N.N. TiO₂-SiO₂ films from organic-free colloidal TiO₂ anatase nanoparticles as photocatalyst for removal of volatile organic compounds from indoor air. *Appl. Catal. B* **2016**, *184*, 119–131. [[CrossRef](#)]
29. Ngoh, Y.S.; Nawi, M.A. Fabrication and properties of an immobilized P25 TiO₂-montmorillonite bilayer system for the synergistic photocatalytic-adsorption removal of methylene blue. *Mater. Res. Bull.* **2016**, *76*, 8–21. [[CrossRef](#)]
30. Wang, P.; Zhou, T.; Wang, R.; Lim, T.T. Carbon-sensitized and nitrogen-doped TiO₂ for photocatalytic degradation of sulfanilamide under visible-light irradiation. *Water Res.* **2011**, *45*, 5015–5026. [[CrossRef](#)] [[PubMed](#)]
31. Kuo, C.Y.; Wu, C.H.; Lin, H.Y. Photocatalytic degradation of bisphenol A in a visible light/TiO₂ system. *Desalination* **2010**, *256*, 37–42. [[CrossRef](#)]
32. Lee, J.M.; Kim, M.S.; Kim, B.W. Photodegradation of bisphenol-A with TiO₂ immobilized on the glass tubes including the UV light lamps. *Water Res.* **2004**, *38*, 3605–3613. [[CrossRef](#)] [[PubMed](#)]
33. Ling, C.M.; Mohamed, A.R.; Bhatia, S. Photodegradation of methylene blue dye in aqueous stream using immobilized TiO₂ film catalyst: Synthesis, characterization and activity studies. *Synthesis* **2007**, *40*, 91–103.
34. Clifton, J.; Leikin, J.B. Methylene blue. *Am. J. Ther.* **2003**, *10*, 289–291. [[CrossRef](#)] [[PubMed](#)]

35. Jawad, A.H.; Shazwani, N.; Mubarak, A.; Azlan, M.; Ishak, M.; Ismail, K.; Nawawi, W.I. Kinetics of photocatalytic decolourization of cationic dye using porous TiO₂ film. *Integr. Med. Res.* **2015**, *10*, 352–362. [[CrossRef](#)]
36. Rizzo, L.; Koch, J.; Belgiorio, V.; Anderson, M.A. Removal of methylene blue in a photocatalytic reactor using polymethylmethacrylate supported TiO₂ nanofilm. *Desalination* **2007**, *211*, 1–9. [[CrossRef](#)]
37. Franco, A.; Neves, M.C.; Carrott, M.M.L.R.; Mendonça, M.H.; Pereira, M.I.; Monteiro, O.C. Photocatalytic decolorization of methylene blue in the presence of TiO₂/ZnS nanocomposites. *J. Hazard. Mater.* **2009**, *161*, 545–550. [[CrossRef](#)] [[PubMed](#)]
38. Ubongchonlakate, K.; Sikong, L.; Saito, F. Photocatalytic disinfection of *Paeruginosa* bacterial Ag-doped TiO₂ film. *Procedia Eng.* **2012**, *32*, 656–662. [[CrossRef](#)]
39. Dong, Y.; Tang, D.; Li, C. Photocatalytic oxidation of methyl orange in water phase by immobilized TiO₂ carbon nanotube nanocomposite photocatalyst. *Appl. Surf. Sci.* **2014**, *296*, 1–7. [[CrossRef](#)]
40. Vezzoli, M.; Martens, W.N.; Bell, J.M. Investigation of phenol degradation: True reaction kinetics on fixed film titanium dioxide photocatalyst. *Appl. Catal. A* **2011**, *404*, 155–163. [[CrossRef](#)]
41. Yang, H.; Zhang, J.; Song, Y.; Xu, S.; Jiang, L.; Dan, Y. Visible light photo-catalytic activity of C-PVA/TiO₂ composites for degrading rhodamine B. *Appl. Surf. Sci.* **2015**, *324*, 645–651. [[CrossRef](#)]



© 2017 by the authors. Licensee MDPI, Basel, Switzerland. This article is an open access article distributed under the terms and conditions of the Creative Commons Attribution (CC BY) license (<http://creativecommons.org/licenses/by/4.0/>).